Journal of King Saud University - Science 36 (2024) 103225

HOSTED BY

Contents lists available at ScienceDirect

Journal of King Saud University - Science

journal homepage: www.sciencedirect.com

Inshights on antifungal potential of *Bryum Argenteum* in association with therapeutical clay smectite and silver nanoparticles

Qaisar Abbas Bhatti [a,b,*], Inam-ul-Haq Qazi [a], M. Fakhar-e-Alam [c], M. Adnan [c], M. Atif [d], Waqas Ali Shah [e], Muhammad Aseer [f], Muhammad Ishaq [a], Komal Seemab [g], Zulfiqar Ali [h]

[a] *Depatment of Chemistry, Faculty of Sciences, Mohi-Ud-Din Islasmic University Nerian Sharif, Azad, Jammu & Kashmir 12010, Pakistan*
[b] *Department of Chemical & life Sciences, Qurtuba University, Dera Ismail Khan, Khyper Pakhtunkhwa, Pakistan*
[c] *Department of Physics, GC University Faisalabad 38000, Pakistan*
[d] *Department of Physics and Astronomy, College of Science, King Saud University, Riyadh 11451, Saudi Arabia*
[e] *Institute of Photovoltaics, University of Stuttgart, Germany*
[f] *Department of Medical Nanotechnology, Tehran University of Medical Sciences, Iran*
[g] *Department of Health, Dera Ismail khan, Khyber PakhtunKhwa, Pakistan*
[h] *Department of Mathematicsand Physics University of Campania luigi Vanvitelli, Viale Abramolincolln,5, 81100 Caserta, Italy*

A R T I C L E I N F O

Keywords:
Bryum argenteum extract
Smectite clay
Silver nanoparticles
Antifungal activity

A B S T R A C T

This work presents the development of a novel antifungal ternary approach that is eco-friendly, biocompatible, and cost-effective. It consists of Bryum argenteum extract, silver nanoparticles, and healing clay smectite. The research focuses on the green production of silver nanoparticles using an aqueous extract of Bryum argenteum as a stabilizing and reducing agent, as well as the synthesis of clay dispersion and plant extract. The silver nanoparticles were characterized by FTIR, SEM, UV–Vis spectroscopy, and XRD. Using a standard phytochemical screening procedure, the aqueous, ethanolic, and acetonic extracts of Bryum argenteum were subjected to phytochemical screening. Silver nanoparticles and plant extract were evaluated for their antioxidant properties using DPPH scavenging activity at 517 nm. Using the agar well diffusion method, a number of investigations have been conducted on the antifungal potential of the proposed innovative ternary approach against Rhizopus oryzae (R. oryzae) and Aspergillus Niger (A. Niger). The color shift validated the silver nanoparticle generation, and the maximum absorbance at 432.11 nm was observed employing UV–Vis spectroscopy. Several functional groups responsible for the synthesis of AgNPs were identified by Fourier transform infrared spectroscopy. The particles are spherical in shape, with the range of 10 nm to 50 nm in size. Both ethanolic and aqueous extracts of Bryum argenteum contain sterols, flavonoids, cardiac glycosides, and terpenoids. AgNPs have stronger antioxidant activity in comparison to the aqueous extract of Bryum argenteum. Out of all the individual components, AgNPs demonstrated the strongest antifungal activity, with clay and plant extract coming in second and third, respectively. Additionally, their binary composition exhibits a synergistic effect with each combination. However, the ternary combination consisting of smectite clay, Bryum argenteum mediated silver nanoparticles, and Bryum argenteum extract showed exceptional antifungal efficiency against the mentioned fungus species. In respect to the zone of inhibition, the maximal antifungal activity was correlated with concentration and pH.
Conclusion: It is concluded here that the proposed ternary system has significant antifungal potential. Future technological and medicinal studies will find this new ternary system to be an invaluable tool.

1. Introduction

Green synthesis of nanoparticles is a widely used technique in practice. It is preferred over physical and chemical processes such as chemical vapor deposition, hydrothermal, sol–gel, and chemical precipitation because of its biodegradable nature, environmentally friendly approach, and use of non-hazardous chemicals (Ying et al., 2022; Zhang et al., 2016).

Concerning green synthesis of nanoparticles, Nanometallics is a popular topic in nanomaterials research and modern material science.

* Corresponding author.
E-mail address: qaisar.abbas@miu.edu.pk (Q. Abbas Bhatti).

https://doi.org/10.1016/j.jksus.2024.103225
Received 9 October 2023; Received in revised form 27 March 2024; Accepted 23 April 2024
Available online 24 April 2024
1018-3647/© 2024 The Authors. Published by Elsevier B.V. on behalf of King Saud University. This is an open access article under the CC BY-NC-ND license (http://creativecommons.org/licenses/by-nc-nd/4.0/).

Because of the unusual surface-to-volume ratio and ability to significantly alter physical, chemical, and biological properties, nanosized metallic particles have been employed in various sectors of life, including electronics, catalysts, dental material development, and pharmaceuticals (Sharma et al., 2009; Zhao et al., 2016). This is why the production and usage of metallic nanoparticles drew the attention of the researchers. Among the noble metal nanoparticles silver nanoparticles are ideal because of their superb optical, thermal electrical properties, catalytic potential, and antimicrobial capabilities(Gurunathan et al., 2015). Owing to their unusual characteristics, AgNPs have found application in a wide range of industries and products, such as pharmaceutical, food, medical device coatings, optical sensors, cosmetics, antibacterial agents, industrial, household, and healthcare products; (Chernousova and Epple, 2013; Key et al., 2022; Li et al., 2014).

The green synthesis of nanoparticles from bryophytes has started in the last decade. Despite being the second-largest (18000–23000 species), believed to be the oldest group of plants still existing in terrestrial habitats, and the closest surviving relative of the early terrestrial plants that have been neglected due to challenges in the collection in a significant amount for analysis; their availability only in certain seasons and their restricted geographical distribution. Research into the medicinal uses of these plants has recently begun. Many genera remain unexplored and offer opportunities for new research(Mukhia et al., 2019; Srivastava and Bhargava, 2022). All regions have bryophytes, which live in aquatic to xeric environments. These plants have higher concentrations of bioactive components like terpenoids, bioflavonoids, isoflavonoids, and flavonoids(Saritas et al., 2001).In contrast to other varieties of non-flowering land plants, these species are a very effective group despite their modest sizes and restricted competitive capacities (Akintola et al., 2020; Alam, 2021).

Members of the Bryaceae family, including *Bryum argenteum*, are widespread throughout the world. Burns, injuries, and wounds are treated with Bryum species and B. argenteum in particular, in folk medicine(Harris, 2008). B. argenteum is reportedly effective against a range of bacterial and fungal strains because it contains proven flavonoids(Karpiński and Adamczak, 2017). With regards to Escherichia coli, Klebsiella pneumoniae, Pseudomonas aeruginosa, Staphylococcus aureus, Enterococcus faecalis, Enterobacter aerogenes, P. syringae, Proteus mirabilis, B. argenteum specifically demonstrated in vitro antimicrobial properties of various (aqueous and ethanolic) extracts (Munir et al., 2023). Additionally, this species has been employed in medicine as an antipyretic, antidotal, and antirhinitic(Iqbal et al., 2019). The antifungal properties of this genus have been proven against fungi like Candida albicans, Trichophyton mentagrophytes and Penicillium ochrochloron (Sabovljevic et al., 2006).

Like phytoremediation, the use of minerals as medicine is ancient. Clays such as smectite, kaolinite and bentonite among minerals are used in various pharmaceutical preparations because of their chemical inertness, rheological properties, large specific surface area, high sorption capacity, and little or no toxicity to the patient(Eren, 2010; Huang et al., 2011; Ngulube et al., 2017).

Smectite refers to a collection of phyllosilicate minerals that includes montmorillonite, beidellite, nontronite, saponite, and hectorite (Odom, 1984). Variations in chemical composition distinguish these and numerous additional less frequent species, including substitutions of Al for Si in tetrahedral cation sites and Al, Fe, Mg, and Li in octahedral cation sites. The effect of di-octahedral smectite in treating epithelium could be predicted due to its delaying property; the attachment of di-octahedral smectite to bacterial strain e.g. Escherichia coli 31A is due to its surface charge, chemical composition, and swelling properties (Bertin et al., 2000).

A novel approach to using a ternary system against human pathogens is suggested, taking into account the individual antimicrobial potential of all three of the aforementioned components. In our previous work (Khan et al., 2022) this approach was applied against selected bacteria by using Bentonite as healing clay. The remarkable outcomes inspired us to apply this strategy to other therapeutic clays and fungi. The current study aims to evaluate the pharmacological properties of the individual components with their unique ternary system, including antioxidant and antibacterial capabilities.

2. Material and methods

2.1. Collection of plant sample

In the month of September 2022, Bryum argenteum was collected from Nerian Sharif in Azad Kashmir, Pakistan, at latitude 33.751608 and altitude 73.7721151(Fig. 1). The plant has been authenticated, and a specimen (Poonch 756) has been submitted to the Herbarium, University of Poonch Rawalakot, Azad Kashmir, Pakistan.

2.2. Materials

Smectite clay, consisting of very fine particles, was supplied by Sigma-Aldrich. It is used as a model substrate. The physicochemical properties of smectite clay are presented in Table 1. Precursor salt silver nitrate ($AgNO_3$-Sigma-Aldrich) and other chemicals like HNO_3, KOH (Sigma-Aldrich) nutrient agar (Pronadisa), potato dextrose agar (Rapid Labs), nutrient broth (Rapid Lab), and deionized distilled water with conductivity less than 0.05 uS were also used. The antifungal Iitraconazole (Sami Pharmaceuticals) served as a reference drug. The overview of this research work is shown in the Fig. 2 and Table 2.

2.3. Methods

2.3.1. Preparation of plant extracts

After collection, the plant was washed first with tap water, then with deionized water to remove dirt particles, and dried after cleaning. Plant material (50 g plant/100 ml distilled water) was boiled for 30 min, resulting in a yellowish aqueous solution. The resulting extract was cooled to room temperature and filtered through Watt-Man filter paper #1. To remove unwanted solid particles, the extract is centrifuged at 5000 rpm for 5 min. A crude extract was then obtained and stored at 4 °C until use.

2.3.2. Ethanolic/Acetonic extract.

An ethanolic/ acetonic extract of shade-dried Bryum argenteum was prepared using a simple maceration procedure. A crude extract of the plant material (50 g) was obtained by grinding it and soaking it in pure ethanol (300 mL) and acetone (300 mL) for fourteen days. The extract

Fig. 1. *Bryum Argenteum* (Silver Moss).

Table 1
Physicochemical Property of Smectite.

Model Adsorbent	Source	ZPC at pH	Primary Particle size (μm)	BET Surface area (m^2/g)	Particle size distribution	Charge on particle
Smectite	Sigma-Aldrich	7.5	0.05 μm	31.09	Narrow	Negative

was then distilled using a Rotavapor model (Rotavapor R-220 Pro), obtained as a crude extract, and kept at 4 °C until use.

2.4. Smectite dispersion

The aqueous dispersion was produced by dispersing 0.1 g of smectite (0.1 % solid content) into 100 ml of Millipore water employing a high-intensity ultrasonic processor, the UP-200, operating at 24 kHz and up to 200 W (Dr Hielscher GmbH) at 22 °C. The dispersion was then examined using various standard experimental techniques(Bhatti et al., 2012).

2.5. Synthesis of Organo-Silver nanoparticles

Mixing Bryum argenteum aqueous extract with $AgNO_3$ solution resulted in a yellowish solution, indicating the synthesis of silver nanoparticles due to the reduction of Ag + into Ag metal. The presence of poly (vinylpyrrolidone) created the stable dispersion of silver nanoparticles in an aqueous medium. The formation of AgNPs was confirmed by UV–VIS spectroscopy (λ_{max}. 432 nm). The sample was observed for 72 h until the highest absorbance was achieved, indicating the completion of the reaction with maximum yield. Various combinations of novel ternary systems comprising an aqueous extract of Bryum argenteum, AgNPs, and smectite clay were prepared to demonstrate their antifungal potential.

2.5.1. Optimum condition for the synthesis of AgNPs

In order to establish optimal conditions for AgNP synthesis, the plant samples were treated with $AgNO_3$ solutions at various ratios, with amounts varying from 0.001 to 0.1 M. UV–Vis spectroscopy was employed to monitor the interaction between the silver ions and the plant extract at various intervals between 0 and 72 h.

2.5.2. Impact of pH on the synthesis of AgNPs

To evaluate the impact of pH (2–10) on the production of AgNPs, the pH of the mixture having an optimum concentration of $AgNO_3$ and plant extract was adjusted using HNO_3 and KOH standard solutions for acidic and basic pH, respectively.

2.5.3. Impact of pH-Dependent time of contact

The impact of the time of contact between $AgNO_3$ solution and plant extract (having a specific pH) on the maximum yield of AgNPs, was studied by applying the standard procedure for pH adjustment.

2.6. Characterization techniques

UV–Vis spectroscopy, FT-IR spectroscopy, scanning electron microscopy, and X-ray diffraction analysis were used to characterize the studied material.

2.6.1. Uv–Vis spectroscopy

To confirm the synthesis of AgNPs from Bryum argenteum aqueous extract, a UV–visible spectrophotometer model (AE Lab. Model AE-S90-UK) with a wavelength range of 190–1100 nm was used at regular intervals.

2.6.2. Scanning electron microscopy

The surface morphology of AgNPs and smectite was examined using a scanning electron microscope (Joel JSM-6490A Analytical Scanning Electron Microscope).

2.6.3. X-ray diffraction

An X-ray diffraction analysis was performed to investigate the elemental composition and sizing of AgNPs and smectite using the Phillips PW 1830 with the specification of a 30 mA current range, a 40 kV voltage, and CuK_1 radiation.

2.6.4. FTIR studies

FTIR spectroscopy was performed to characterize smectite and AgNPs in the range of 4000 cm^{-1} to 500 cm^{-1} using the FTIR spectrometer (SPECORD 210 PLUS).

2.6.5. Point of zero charge (ZPC) as a function of PH

To determine the point of zero charge of smectite as a function of pH, the potentiometric titration technique was applied using the Denver potentiometer (USA 250).

2.7. Antifungal activity

The fungal strains used in this assay are Aspergillus niger (A. niger) and Rhizopus oryzae (R. oryzae), and the agar well diffusion method is used. When the medium reached a temperature of 30–40 °C and was well mixed, about 1 ml of the inoculum was poured into the sterilized potato dextrose agar medium, and 20 ml of this medium was poured into all Petri dishes and allowed to solidify. Four 6 mm indentations were made using a sterile cork borer. In each petri dish, 50 μL of the plant extract was poured into each well using a sterilized micropipette. Negative controls (DMSO) were maintained for each fungal strain where neat solvents were used instead of the extract. The control areas were subtracted from the test zones. The standard anti-mycotic, Itraconazole (25 μg/mL) was used as a positive control. Plates were incubated at 28 °C for 48–72 h. The diameter of the zone of inhibition was measured to estimate the growth of fungus. The entire process of horizontal laminar airflow was performed aseptically. The experiment was performed in triplicate.

2.8. Antioxidant activity

Using the scavenging potential of DPPH free radicals, an extract of silver nanoparticles was evaluated for an antioxidant assay. (5–20 mg/ml), ethanol, the aqueous extract, and its silver nanoparticles were mixed. The addition of the DPPH solution and shaking was done. The mixture was kept in the dark for 30 min. A UV spectrophotometer (Cecil-Elect. UK) at 517 nm was employed against a blank (1 mL ethanol + 0.5 mL DPPH solution) to determine the optical density of each sample. Readings were taken three times for each sample. The formula determines optical density as follows

$$Inhibition(\%) = [(A_B - A_A)/A_B] \times 100 \quad (1)$$

2.9. Phytochemical screening

To identify the natural compounds present in different extracts, a phytochemical screening was performed on aqueous, methanolic, and ethanolic extracts of Bryum argenteum using standard methods.

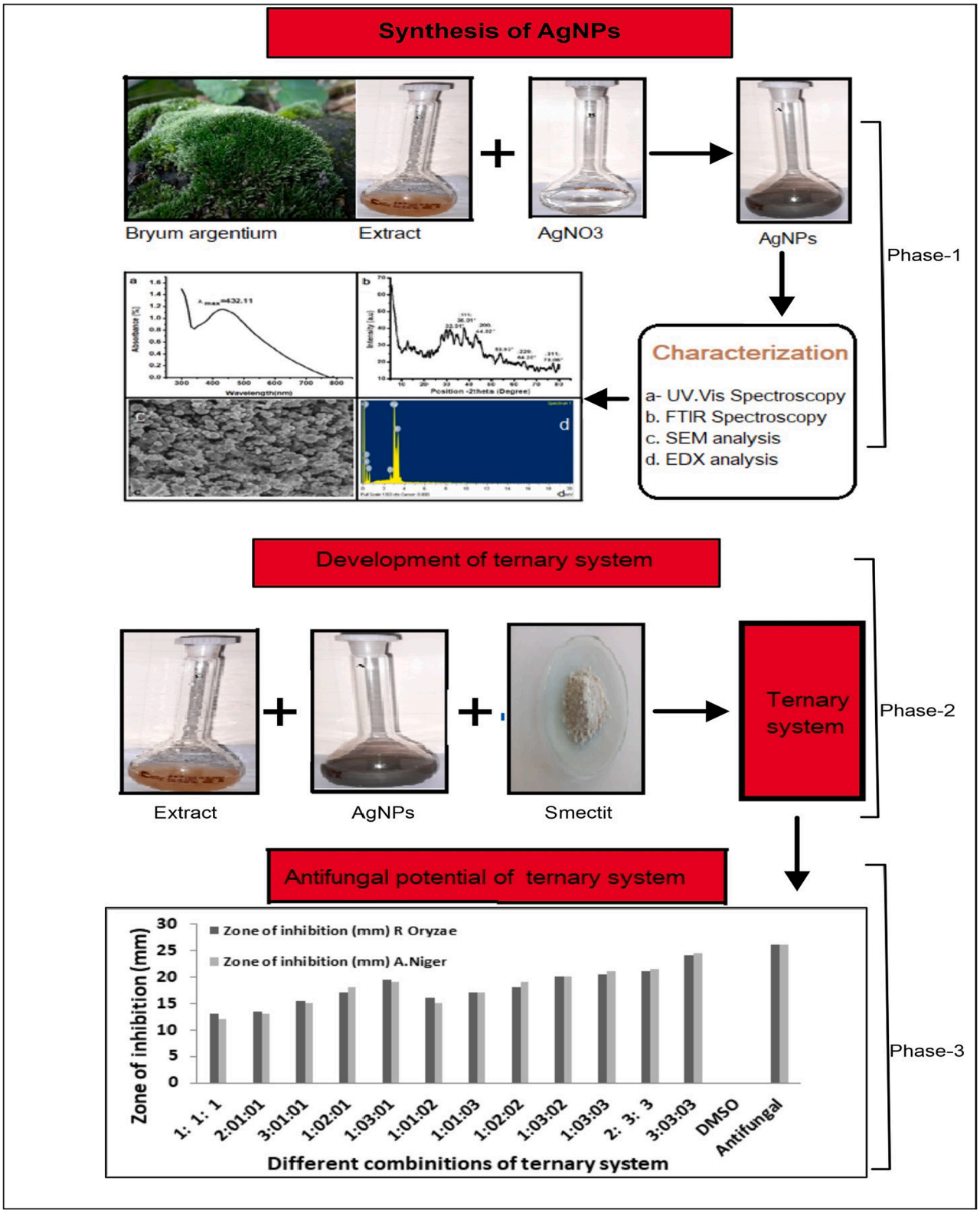

Fig. 2. Overview of the research work.

3. Results and discussion

3.1. Characterization of smectite

Smectite clay, a member of the layered silicates known as hydroxyl alumino-silicates, contains alkali and alkaline earth metals. Smectite purchased from Sigma has been characterized in terms of its size, surface charge, purity, and surface area. Some of the physicochemical properties of smectite are given in Table 1.

The structure of smectite contains tetrahedral layers arranged between octahedral layers in the clay stack pattern. The SEM image of smectite shown in Fig. 3a examines the shape and structure of the

Table 2
Phytochemical screening of different Extracts of *Bryum Argenteum.*

Compound	Photochemical Test applied	Observation	Aqueous extract	Ethanolic Extract	Acetonic Extract
Alkaloids	Mayers and hagers test	No ppt	−	−	−
Anthraquinones	Born Trager's test	No layer formation	−	−	−
Flavanoids	Lead acetate test and gelatin test	White ppt	+	+	+
Sterols	Alkaline reagent and sodium hydroxide test Salkowaski test	Yellow fluorescent colour Reddish brown colour	+	+	+
Terpenoids	Libermann-burchardt test Salkowiski test	Brown ring The lower layer turned yellow Deep red colour	+	+	+
Saponins	Libermann-burchardt test Phenyl hydrazine test Froth test	Yellow-orangecolour No froth	−	−	−
Cardiac Glycosides	Keller killeni test Ferric chloride test	Brown ring Green colour	+	+	+

material.

The literature reveals that smectite consists of two-dimensional layers of octahedral AlO_4 or tetrahedral SiO_4 at the corner with the chemical formula $Al_2Si_3O_4$. The silica tetrahedron shares its three oxygen atoms with the next tetrahedron, while the oxygen at the fourth corner is not shared with the other tetrahedron(Bertin et al., 2000; Odom, 1984). All of the oxygen from the undivided apex is going in the same direction as the bed. Made from cations such as aluminum or magnesium, the octahedral sheets are fixed in clays by tetrahedral sheets. Six oxygen atoms are coordinated on this octahedron sheet. The undivided apex of the tetrahedron leaves forms one side of the octahedron leaves. A gap above the tetrahedron sheet has an extra oxygen atom. The bond formation occurs between additional oxygen and hydrogen atoms, creating an OH group in the clay structure. A single octahedral and tetrahedral group exists in a 1:1 tone; similarly, two tetrahedral and one octahedral group exist in a 2:1 tone. The layers can be neutrally or net negatively charged depending on the composition of the tetrahedral and octahedral layers. Interlayer cations such as Na + and K + take over the balancing of negative charges. Hence, it is evident that smectite consists of silicate and aluminate groups in an arrangement called the TOT structure. The space between the TOT layers contains water molecules and cations(Bertin et al., 2000).

3.1.1. Particle size

The average particle size quantified by XRD analysis was 0.05 μm. A narrow particle size distribution was noticed from the peak values and computation using the Scherer equation.

$$\tau = \frac{K\lambda}{\beta\cos\theta} \quad (2)$$

where τ the average size of the crystalline domains,K is a dimensionless shape factor, with a value close to unity. λ, is the wavelength of the X-ray, β, is the line broadening at half the maximum intensity (FWHM) and θ is the Bragg angle.

3.1.2. Point of zero charge (ZPC) as a function of pH

The potentiometric titration technique as a function of pH was used to determine the point of zero charges. A potentiometer (HANNA H1931) was used for this purpose. The ZPC was calculated at pH 7.5.

3.1.3. Scanning electron microscopy

SEM was employed to investigate the surface morphology of smectite clay. Fig. 2a exhibits an SEM image of clay. It is observed that smectite has 2-D sheets having honeycomb texture.

3.1.4. FTIR studies

The FTIR spectrum of clay is presented in Fig. 3b. The absorption peaks reported in FTIR spectroscopic measurements are 1633 cm^{-1} and 3626 cm^{-1} due to vibrations of OH groups in the smectite due to stretching and bending vibrations of adsorbed water molecules. The bands of the OH group, AlMgOH, Al_2OH, and AlFeOH, can be given as 875, 916, and 835 cm^{-1}. The 530 cm^{-1} and 1032 cm^{-1} bands are due to Si-O-Si stretching and Si-O strain. The octahedral layer with Al gives the most sensitive band at 515 cm^{-1}. The SiOH group gave a broad band near 995 cm^{-1}(Madejová et al., 2002).

3.2. Characterization of silver nanoparticles

UV–Vis spectroscopy was performed for absorbance measurements in the range of 190 nm to 1100 nm. No early-stage peak showed any synthesis of Ag particles, but surface plasmon resonance of silver was observed after half an hour and synthesis of AgNPs was confirmed by an intense absorption peak at λ_{max}. 432 nm (Fig. 4a). Reduction of Ag^{+}in to AgNPs with the help of plant secondary metabolites(The plant extract served as both reducing and stabilizing agents)completed in 72 h, shown by maximum absorbance at mentioned λ_{max}.In order to find the optimum concentration of plant extract an analysis of plant extracts in different volume ratios of 10 mL to 30 mL with a fixed volume(10 mL) of $AgNO_3$ having concentrations from 0.001 to 0.1 M at room temperature was performed(Rucha et al., 2012).

3.2.1. Scanning electron microscopy

SEM was employed to investigate the surface morphology of silver nanoparticles. Fig. 4b exhibits the SEM image of silver nanoparticles in different diameters. The particles are spherical in shape with the range of 10 nm to 50 nm in size.

3.2.2. XRD analysis of Ag nanoparticles

To determine the size and crystallinity of silver nanoparticles, XRD analysis was performed. Fig. 4c and 4d list the XRD patterns of the

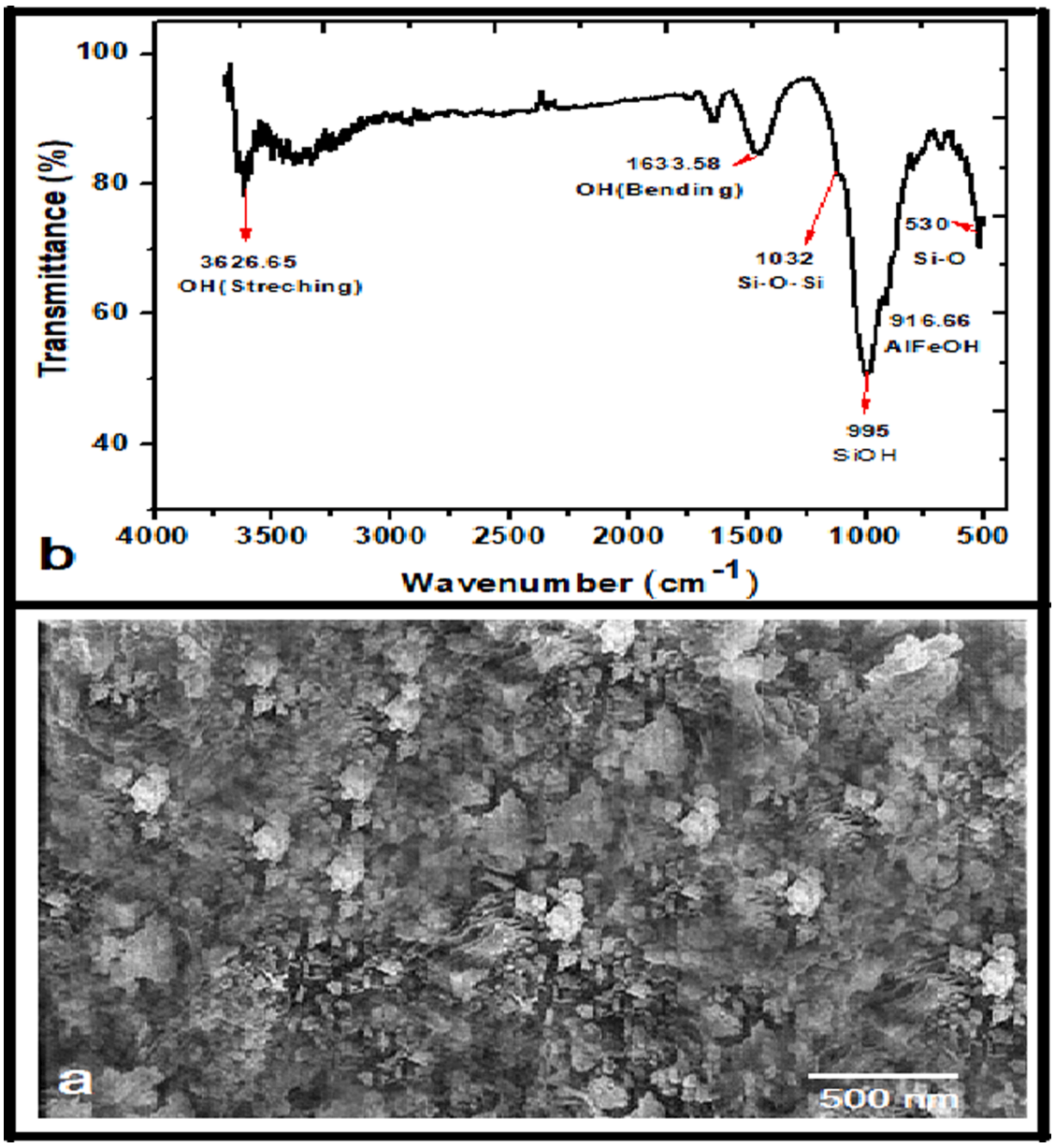

Fig. 3. a. SEM Picture of smectite b. FTIR Spectrum of Smectite.

synthesized AgNPs. The X-ray diffraction peaks at 2θvalues 38.01°, 44.21°, 64.4°, and 78.01° with d-spacing of 2.467, 5.7658, and 2.922, corresponded to the hkl plans of (111), (200), (220), and (311) respectively, showed the production of silver nanoparticles as shown in Fig. 3c,3d (Zielińska et al., 2009).

3.3. Optimum conditions for the synthesis of AgNPs

To establish ideal conditions for AgNPs fabrication at ambient temperature, $AgNO_3$ solutions in concentrations ranging from 0.001-0.1 M were applied to the plant extract in various volume ratios i.e. 10 to 30 mL. UV–visible spectroscopy was used to track the reaction between the metal ion and plant extract over durations ranging from 0 to 72 h. The surface Plasmon absorption band displayed exceptional efficiency at λmax 432 nm, indicating that AgNPs are synthesized swiftly and steadily over 72 h. The graph demonstrated how increasing $AgNO_3$ concentration led to an increase in AgNP production. Maximum AgNPs production was observed at 0.1 M $AgNO_3$ for 30Ml of plant extract (Ishii and Xuan, 2014; Ndikau et al., 2017).

3.3.1. Impact of pH on the synthesis of silver nanoparticles

As pH rises, the percentage absorption rises as well. Both the synthesis of AgNPs and the reduction of particle size are indicated by the growth and shift of the absorption band to a longer wavelength, respectively. The highest absorbance was observed as a narrow peak at pH 10, which is an indication of maximum synthesis and uniform particle size distribution. Therefore, it is believed that the basic pH values promote AgNPs synthesis as well as a decrease in particle size and particle size distribution and vice versa (Alqadi et al., 2014a; Awada et al., 2020). The effect of pH on AgNPs synthesis is given in the supplementary data file.

3.3.2. Impact of time-dependent pH

The effect of time-dependent pH on AgNPs synthesis is also given in the supplementary data file. When the plant extract and $AgNO_3$ solution come into contact for a longer period and the pH rises, the percentage absorbance increases. The results showed that a maximum absorbance was observed after 72 h with pH 10. Consequently, it is believed that the pH-10 and 72-hour contact time; control both the synthesis of AgNPs

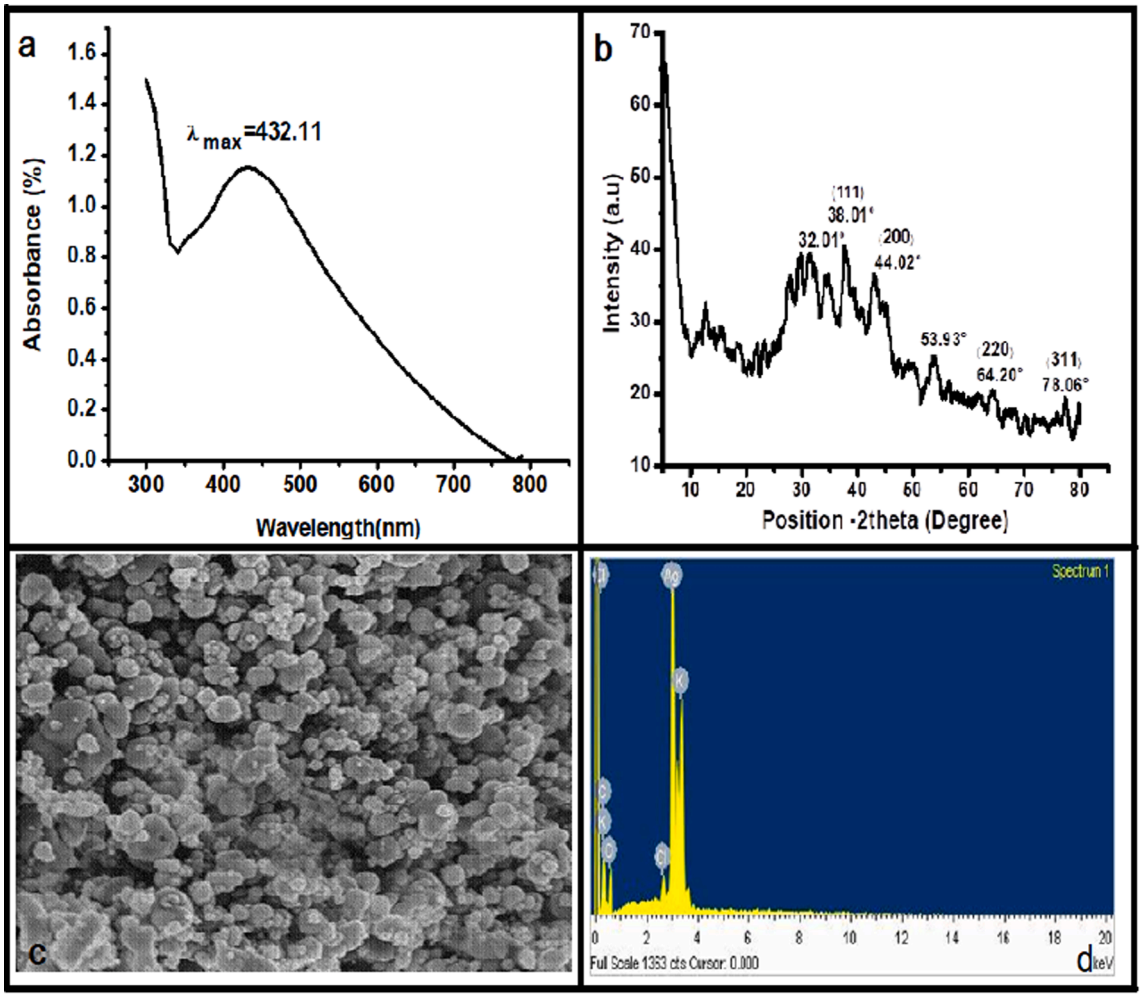

Fig. 4. a.UV.Vis-Spectrum of Silver Nanoparticles b. SEM of Silver Nanoparticles c. XRD Graph of Silver Nanoparticles d. Energy diagram of AgNPs.

and particle size.(Alqadi et al., 2014b; Awada et al., 2020; Darroudi et al., 2011).

3.4. Phytochemical screening

Different bioactive components present in *Bryum argenteum* are shown in the tabulated form. Along with other phytochemicals presence of flavonoids is confirmed(Mccleary et al., 1960; Saritas et al., 2001). Our results are in good agreement with those reported in the literature (Karpiński and Adamczak, 2017; Mccleary et al., 1960; Saritas et al., 2001).

3.5. Antioxidant activities of AgNPs and Bryum argenteum

DPPH$^{\bullet}$ is commonly used for investing free radical scavenging properties of natural compounds and nano particles. *Bryum argenteum* extract scavenged 14.65, 8.34, 7.61, 6.96,5.15 and 1.74 % DPPH radicals at concentrations 400, 300, 200, 100, 50, 25 μg/mL, whereas AgNPs scavenged 86.75, 82.19, 76.15, 61.58, 51.65 and 37.08 % for the same concentrations. According to this study, the antioxidant activity of silver nanoparticles surpasses the activity of the *Bryum argenteum* extract. Fig. 5 compares the two, i.e. the extract of *Bryum argenteum* and the silver nanoparticles(Akintola et al., 2020; Fukumoto and Mazza, 2000; Zhang et al., 2017).

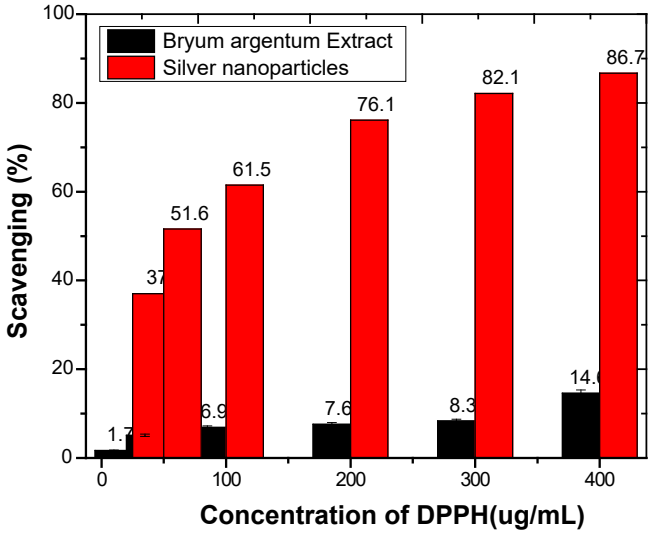

Fig. 5. Comparisons between the Antioxidant Activity of Bryum Argenteum and Silver Nanoparticles.

3.6. Antifungal assays

The antifungal potential of individual components in binary and ternary systems has been evaluated in aqueous, ethanolic, and acetonic systems.

3.6.1. Antifungal potential of individual components

A systematic, precise antifungal investigation was conducted to assess the antifungal potential of the proposed ternary system. This study comprised an investigation of the antifungal potential of the individual, binary system, and finally, the ternary system.

AgNPs, smectite dispersion, and plant extract each showed antifungal activity in an aqueous solution, with 10, 18, and 13 mm zones of inhibition against A. Niger, accordingly. The same components exhibited an 8, 16, and 12 mm zone of inhibition in the case of R. oryzae, respectively. But compared to R. oryzae, this antifungal potential is higher against A. niger (Sabovljevic et al., 2006). These findings revealed that the order of antifungal potential of individual components is as follows:

AgNPs > Smectite clay dispersion > Aqueous plant extract.

For ethanolic media, the zones of inhibition exhibited by plant extract, AgNPs, and clay for A.niger were 14, 21, and 18 mm, respectively, while for R. oryzae they were 12, 22, and 12 mm, respectively. According to the findings, AgNPs in the ethanolic medium have a higher

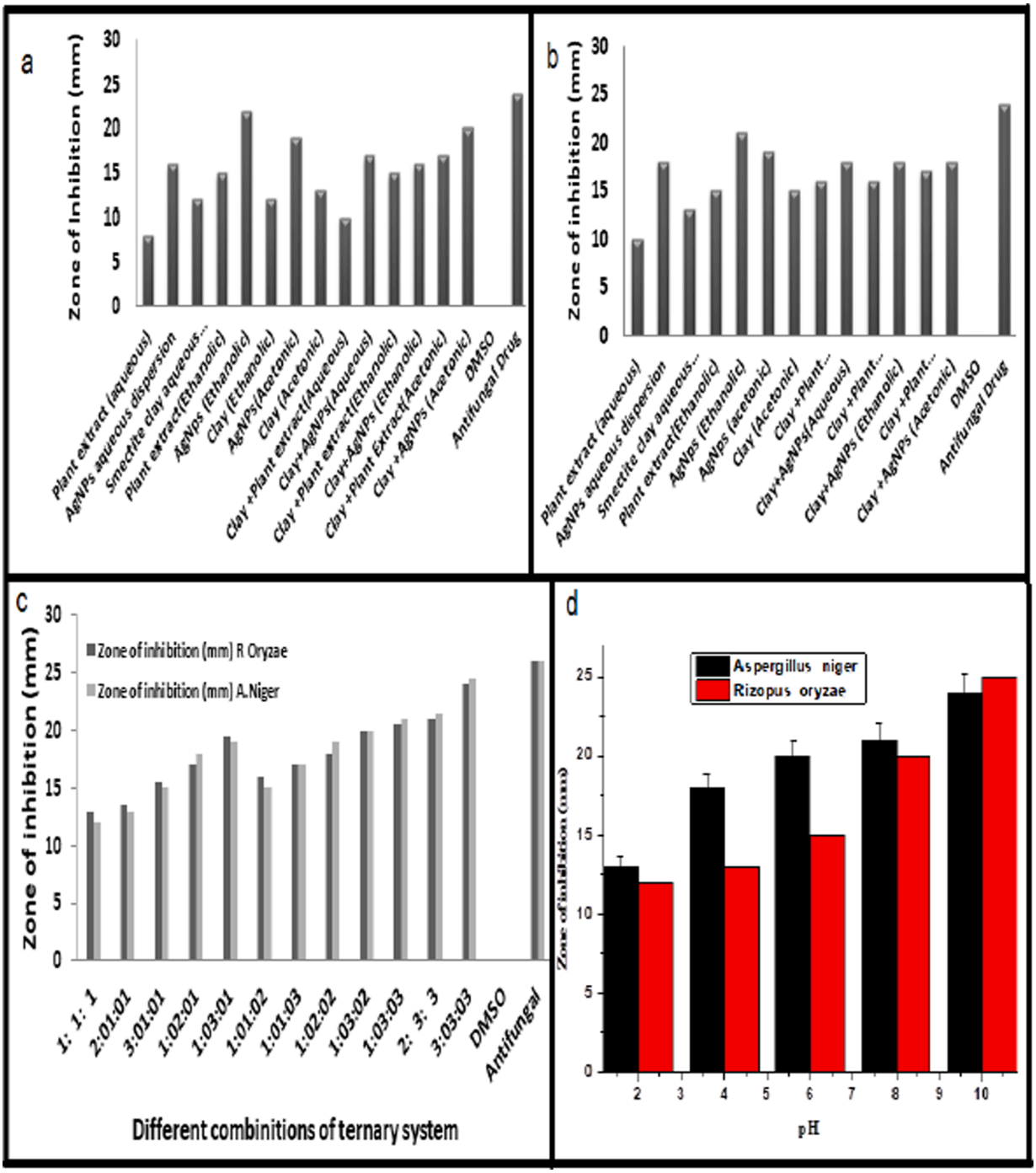

Fig. 6. A. Antifungal activities of Individual and Binary system for A.Niger**b.**R.Oryzae **c.**Comparison of Antifungal Activity of Novel Ternary System Comprising of*Bryum argenteum*, AgNPs and Smectite Clay Against A.Nigar an R. Oryzae**d**. Effect of pH on Zone of Inhibition at Antifungal Activity.

potential for antifungal activity than clay and plant extracts(Sabovljevic et al., 2006). However, the overall potential of each component was higher than that of the components in the aqueous medium. This is caused by the components' inherent potential in addition to the medium's antibacterial activity (Sabovljevic et al., 2006). The findings are shown in Fig. 6a.

The order of antifungal potential of individual components in the ethanolic medium is as under.

AgNPs > smectite clay dispersion > aqueous plant extract.

Antifungal potential of individual components in acetonic medium followed the following order.

Smectite clay dispersion > AgNPs > aqueous plant extract.

However, the values of the zone of inhibitions were higher for R. oryzae as compared to A. niger. The overall order of antifungal potential depending upon the nature of the medium is as under.

Ethanolic medium >acetonic medium >aqueous medium.

The results are depicted in Table 3 for A. niger, and Table 4 for R. oryzae respectively. These results are also shown in Fig. 6b.

3.6.2. *Antifungal potential of binary systems*

Antifungal potential of the binary system comprising of clay and plant extract and clay coupled with AgNPs in an aqueous medium showed 16 and 18 mm zone of inhibition against *A. niger* respectively while in the case of R. Oryzae, same binary system exhibited a 10 and 17 mm zone of inhibition. These findings revealed that the order of antifungal potential of the binary system is as under.

Clay + AgNPs > Clay + plant extract.

However, this antifungal potential is higher against A. Niger. From these results, it is also observed that clay coupled with AgNPs showed a synergistic effect and did not suppress the antifungal potential of each other.

The binary system comprising clay and plant extract and clay coupled with AgNPs in ethanolic medium showed 16 and 18 mm zone of inhibition against A. Niger respectively while in the case of *R. oryzae,* same binary system exhibited a 15 and 16 mm zone of inhibition. It is revealed that the order of antifungal potential of the binary system in the ethanolic medium is as follows.

Clay + AgNPs >Clay + plant extract.

The case of an acetonic medium binary system comprising clay and plant extract and clay coupled with AgNPs showed a 17 and 18 mm zone of inhibition against A. Niger respectively while in the case of R. Oryzae, same binary system exhibited an 18 and 20 mm zone of inhibition. These findings revealed that the order of antifungal potential of the binary system in the acetonic medium is the same as that of the ethanolic medium.

The overall order of antifungal potential of the binary system comprising of clay and AgNPs independence of medium is as under.

Acetonic medium > Ethanolic medium >Aqueous medium.

The Results for the mentioned binary systems are also shown in Table 3 for *A.niger*, and its comparison with the literature cited(Khan et al., 2022)and in Table 4 for *R.oryzae*and its comparison with the literature cited(Khan et al., 2022)respectively.

Table 3
Antifungal activities of Bryum Argenteum, AgNPs and smectite clay for A.niger and and its comparison with the literature cited(Khan et al., 2022).

S. No	Samples used	zone of inhibition (mm) for A.Nigar (Khan. M et al., 2022)	zone of inhibition (mm) for A.Nigar (Khan. M et al., 2022)
1	Plant extract (aqueous)	**10**	**2**
2	AgNPs aqueous dispersion	**18**	**14**
3	Smectite clay aqueous dispersion	**13**	**1**
4	Plant extract (Ethanolic)	**15**	**10**
5	AgNps (Ethanolic)	**21**	**20**
6	AgNps (acetonic)	**19**	**20**
7	Clay (Acetonic)	**15**	**1**
8	Clay + Plant extract (Aqueous)	**16**	**1**
9	Clay + AgNPs (Aqueous)	**18**	**14**
10	Clay + Plant extract (Ethanolic)	**16**	**12**
11	Clay + AgNPs (Ethanolic)	**18**	**21**
12	Clay + Plant Extract (Acetonic)	**17**	**3**
13	Clay + AgNPs (Acetonic)	**18**	**7**
14	DMSO	**0**	**0**
15	Antifungal Drug	**24**	**25**

Table 4
Antifungal activities of Bryum Argenteum, AgNPs and Smectite Clay for R. Oryzaeand itscomparison with literature cited(Khan et al., 2022).

S. No	Samples used	zone of inhibition (mm) for R.Oryzae (Khan.M et al., 2022)	zone of inhibition (mm) for R.Oryzae (Khan.M et al., 2022)
1	Plant extract (aqueous)	**8**	**1**
2	AgNPs aqueous dispersion	**16**	**16**
3	Smectite clay aqueous dispersion	**12**	**1**
4	Plant extract (Ethanolic)	**13**	**12**
5	AgNps (Ethanolic)	**22**	**20**
6	AgNps (acetonic)	**13**	**20**
7	Clay (Acetonic)	**19**	**1**
8	Clay + Plant extract (Aqueous)	**16**	**2**
9	Clay + AgNPs (Aqueous)	**18**	**16**
10	Clay + Plant extract (Ethanolic)	**15**	**13**
11	Clay + AgNPs (Ethanolic)	**19**	**21**
12	Clay + Plant Extract (Acetonic)	**18**	**3**
13	Clay + AgNPs (Acetonic)	**19**	**7**
14	DMSO	**0**	**0**
15	Antifungal Drug	**24**	**25**

Table 5a
Antifungal Activity of Novel Ternary System *Bryum argenteum* AgNPs and Smectite clay for A.niger.

Novel Ternary system	Samples used	% zone of inhibition (mm)
Extract:AgNPs:Smectite*A.Niger*		
Novel ternary system of *Bryum argenteum*, AgNPs and Smectite clay	**1: 1: 1**	**12**
	2: 1: 1	**13**
	3: 1: 1	**15**
	1: 2: 1	**18**
	1: 3: 1	**19**
	1: 1: 2	**15**
	1: 1: 3	**17**
	1: 2: 2	**19**
	1: 3: 2	**20**
	1: 3: 3	**21**
	2: 3: 3	**21.5**
	3: 3: 3	**24.5**
	DMSO	**0**
	Antifungal Drug	**26**

3.6.3. Antifungal potential of ternary systems

To evaluate not only the antifungal potential of the ternary system but the synergetic or antagonistic impact of each component, twelve different combinations were prepared as shown in Table 5a for A. niger and Table 5b for R.oryzae respectively.

According to the table, the antifungal potential of the ternary system increases as the concentration of AgNPs increases. For instance, in the case of A. niger, the zone of inhibition increased up to 19 mm for 1:3:1 and 1:1:1 (12 mm), respectively. Increasing the concentration of the remaining two components produced outcomes that were comparable. These findings showed that while each component had a unique contribution to antifungal activity, the component with the larger contraction increased antifungal activity overall. The antifungal activity of AgNPs is well known, so this finding is not unexpected. However, since both plant extract and swelling clay are used as antifungal dispersants and carriers respectively for AgNPs to provide chances of interacting with fungal strains, their importance cannot be ignored. This argument is also further supported by the results obtained by increasing the concentration (threefold) of all components of the ternary system. The antifungal activity also increased to its maximum i.e. 24.5 mm for A. niger and 24 mm for R.oryzae, Here the role of healing clay smectite and plant extract can easily be observed. Due to the physical parameters of bentonite like high cation exchange capacity, high surface area, high swelling capacity, high water dispersibility, high absorption capacity, and non-toxic nature(Dardir et al., 2018) astringent and hemostatic action(Carretero, 2002)they are typically used in medicinal and cosmetic uses. Keeping in view the mentioned properties of clay we can easily understand this increase in antifungal activity. Antifungal activity of the Bryum argenteum has also been proven by literature(Motti et al., 2023; Sabovljevic et al., 2006). Therefore when these three components were gathered in a suggested ternary system these components showed a synergistic effect. The result of antifungal activities of the ternary system against A. niger and R.Oryzae are shown in Tables 5a and 5b respectively.

From the table, it is also observed that the presence of plant extract showed an antagonistic effect in the ternary system as shown by the 1:1:1 (13 mm), 2:1:1(13.5 mm) and 3:1:1 (16 mm) respectively. In our study, the ternary system with a ratio of 3:3:3 showed a marked effect in controlling the growth of selected fungal strains i.e. (24.5 mm for A. niger and 24 mm for R.Oryzae as shown in Fig. 6c.

Silver nanoparticles are found in higher concentrations than other composite ternary systems, and their antimicrobial activity varies depending on the microbial organism(Elmer et al., 2005). Silver nanoparticles can significantly delay mycelial growth in vitro and can bind directly to and penetrate the cell membrane to destroy spores. The diffusion mechanism of silver nanoparticles into the microbial cell membrane is not fully understood(Park et al., 2013). This study found that silver nanoparticles, Bryum argenteum extract and smectite clay were effective in regulating two phytopathogens, A.niger and R. oryzae, as a fungicide surrogates. The ternary system strongly inhibited the growth of fungi, suggesting the possibility of eradicating them using the method.

However, for practical implementation, parameters such as phytotoxicity and delivery to the host tissue must be evaluated.

Table 5b
Antifungal Activities of Novel Ternary System *Bryum argenteum* AgNPs and Smectite Clay for R. oryzae.

Novel Ternary system	Samples used	% zone of inhibition (mm)
Extract:AgNPs: Smectite R Oryzae		
Novel ternary system of*Bryum argenteum*AgNPs and Smectite clay	**1: 1: 1**	**13**
	2: 1: 1	**13.5**
	3: 1: 1	**15.5**
	1: 2: 1	**17**
	1: 3: 1	**19.5**
	1: 1: 2	**16**
	1: 1: 3	**17**
	1: 2: 2	**18**
	1: 3: 2	**20**
	1: 3: 3	**20.5**
	2: 3: 3	**21**
	3: 3: 3	**24**
	DMSO	**0**
	Antifungal Drug	**26**

3.6.4. Effect of pH on antifungal activity

Table 6 displays the antimicrobial behavior of silver nanoparticles mediated by *Bryum argenteum* at various pH values. As pH rises, antifungal action rises as well. AgNPs production grows as the medium's pH rises, as was previously stated in Section 3.3.1, but particle size reduces (Ndikau et al., 2017). In comparison to larger particles, smaller particles can more readily interact with the fungal cell membrane and penetrate the cell, increasing antifungal activity. At neutral pH, the findings are comparable to those produced by individual AgNPs, but at higher pH, the higher values of the zone of inhibition are caused by the medium's highly basic and corrosive character(Wiegand et al., 2015). The result is presented in Fig. 6d.

4. Conclusion

This study supports the presence of flavonoids, sterols, terpenoids, and cardiac glycosides in B. argenteum as significant secondary metabolites. Together with medicinal clay, these bioactive substances and silver nanoparticles demonstrated antifungal activity against A. niger and R. Oryza. This research was done to find out how well three different components in a ternary system, namely H. Bryum argenteum extract, Bryum argenteum silver nanoparticles, and a smectite clay, worked together. According to this research, ternary systems can be utilized as natural fungicides rather than synthetic antifungals.

This study supports the presence of flavonoids, sterols, terpenoids and cardiac glycosides as important secondary metabolites in *B. argenteum*. Together with medicinal clay, these bioactive substances and silver nanoparticles demonstrated antifungal activity against A. niger and R. oryzae. All three components showed the antifungal potential against selected fungal strains, however higher antifungal potential was observed by AgNPs as an individual component. In the case of the binary system, clay + AgNPs showed the maximum antifungal activity. While the presence of these components in the suggested ternary system showed the highest antifungal potential, this is comparable to the standard antifungal drug. It is also observed that antifungal activity is pH and concentration-dependent. This study suggests that the ternary system can be used as an antifungal instead of a synthetic fungicide.

CRediT authorship contribution statement

Qaisar Abbas Bhatti: Writing – original draft, Writing – review & editing. **Inam-ul-Haq Qazi:** Conceptualization. **M. Fakhar-e-Alam:** Resources. **M. Adnan:** Resources. **M. Atif:** Validation. **Waqas Ali Shah:**

Table 6
Effect of pH on Zone of Inhibition at Antifungal Activity.

pH	Fungal strains	
	Aspergillus Niger(mm)	***Rizopus Oryzae (mm)***
2	**13**	**12**
4	**18**	**13**
6	**20**	**15**
8	**21**	**20**
10	**24**	**25**
Control	**28**	**28**

Writing – review & editing. **Muhammad Aseer:** Formal analysis. **Muhammad Ishaq:** Formal analysis. **Komal Seemab:** Investigation, Visualization. **Zulfiqar Ali:** Formal analysis, Investigation.

Declaration of competing interest

The authors declare that they have no known competing financial interests or personal relationships that could have appeared to influence the work reported in this paper.

Acknowledgement

Researchers Supporting Project number (RSP2024R397), King Saud University, Riyadh, Saudi Arabia

Appendix A. Supplementary material

Supplementary data to this article can be found online at https://doi.org/10.1016/j.jksus.2024.103225.

References

Akintola, A.O., Kehinde, B.D., Ayoola, P.B., Adewoyin, A.G., Adedosu, O.T., Ajayi, J.F., Ogunsona, S.B., 2020. Antioxidant properties of silver nanoparticles biosynthesized from methanolic leaf extract of Blighia sapida. IOP Conf. Ser. Mater. Sci. Eng. 805, 012004 https://doi.org/10.1088/1757-899X/805/1/012004.

Alam, A., 2021. Article Info Ar tic le histo ry Potential of bryophytes in prevention and medication of COVID-19 Annals of Phytomedicine, Volume10, Special Issue1 (COVID-19): S121-S129, 2021 Annals of Phytomedicine: An International Journal http://www.ukaazpublications.com/publications/index.php. Doi: 10.21276/ap.covid19.2021.10.1.12.

Alqadi, M.K., Noqtah, O.A.A., Alzoubi, F.Y., Alzouby, J., Aljarrah, K., 2014a. pH effect on the aggregation of silver nanoparticles synthesized by chemical reduction. SpringerMK Alqadi, OA Abo Noqtah, FY Alzoubi, J Alzouby, K AljarrahMaterials Science-Poland, 2014•Springer 32, 107–111. Doi: 10.2478/s13536-013-0166-9.

Alqadi, M.K., Noqtah, O.A.A., Alzoubi, F.Y., Alzouby, J., Aljarrah, K., 2014b. pH effect on the aggregation of silver nanoparticles synthesized by chemical reduction. SpringerMK Alqadi, OA Abo Noqtah, FY Alzoubi, J Alzouby, K AljarrahMaterials Science-Poland, 2014•Springer 32, 107–111. Doi: 10.2478/s13536-013-0166-9.

Awada, C., Micromachines, H.T.-, 2020, undefined, 2020. Effect of pH and nanoparticle capping agents on Cr (III) monitoring in water: A kinetic way to control the parameters of ultrasensitive environmental detectors. mdpi.comC Awada, H TraboulsiMicromachines, 2020•mdpi.com 11, 1–14. Doi: 10.3390/mi11121045.

Bertin, Y., Girardeau, J.P., Darfeuille-Michaud, A., Martin, C., 2000. Epidemiological study of pap genes among diarrheagenic or septicemic Escherichia coli strains producing CS31A and F17 adhesins and characterization of Pap(31A) fimbriae. J. Clin. Microbiol. 38, 1502–1509. https://doi.org/10.1128/JCM.38.4.1502-1509.2000.

Bhatti, Q.A., Baloch, M.K., Schwarz, S., Petzold, G., 2012. Impact of Various Parameters Over the Adsorption of Polyvinylpyrrolidone onto Kaolin. J. Dispers. Sci. Technol. 33, 1739–1745. https://doi.org/10.1080/01932691.2011.629530.

Carretero, M.I., 2002. Clay minerals and their beneficial effects upon human health a review. Appl. Clay Sci. 21, 155–163. https://doi.org/10.1016/S0169-1317(01)00085-0.

Chernousova, S., Epple, M., 2013. Silver as antibacterial agent: Ion, nanoparticle, and metal. Angewandte Chemie - International Edition 52, 1636–1653. https://doi.org/10.1002/ANIE.201205923.

Dardir, F.M., Mohamed, A.S., Abukhadra, M.R., Ahmed, E.A., Soliman, M.F., 2018. Cosmetic and pharmaceutical qualifications of Egyptian bentonite and its suitability as drug carrier for Praziquantel drug. Eur. J. Pharm. Sci. 115, 320–329. https://doi.org/10.1016/J.EJPS.2018.01.041.

Darroudi, M., Ahmad, M.B., Zamiri, R., Zak, A.K., Abdullah, A.H., Ibrahim, N.A., 2011. Time-dependent effect in green synthesis of silver nanoparticles. Int. J. Nanomed. 6, 677–681. https://doi.org/10.2147/IJN.S17669.

Elmer, R.A.G., Hoyte, S.M., Vanneste, J.L., Reglinski, T., Wood, R.N., Parry, F.J., 2005. Biological control of fruit pathogens. New Zealand Plant Protection 58, 47–54. https://doi.org/10.30843/NZPP.2005.58.4253.

Eren, E., 2010. Adsorption Performance and Mechanism in Binding of Azo Dye by Raw Bentonite. Clean (Weinh) 38, 758–763. https://doi.org/10.1002/CLEN.201000060.

Fukumoto, L.R., Mazza, G., 2000. Assessing antioxidant and prooxidant activities of phenolic compounds. J. Agric. Food Chem. 48, 3597–3604. https://doi.org/10.1021/JF000220W.

Gurunathan, T., Mohanty, S., Nayak, S.K., 2015. A review of the recent developments in biocomposites based on natural fibres and their application perspectives. Compos. A Appl. Sci. Manuf. 77, 1–25. https://doi.org/10.1016/J.COMPOSITESA.2015.06.007.

Harris, E.S.J., 2008. Ethnobryology: traditional uses and folk classification of bryophytes. Doi: 10.1639/0007-2745(2008)111[169:ETUAFC]2.0.CO;2 111, 169–217. Doi: 10.1639/0007-2745(2008)111.

Huang, R., Wang, B., Yang, B., Zheng, D., Zhang, Z., 2011. Equilibrium, kinetic and thermodynamic studies of adsorption of Cd(II) from aqueous solution onto HACC–bentonite. Desalination 280, 297–304. https://doi.org/10.1016/J.DESAL.2011.07.033.

Iqbal, S., Fakhar-e-Alam, M., Akbar, F., Shafiq, M., Atif, M., Amin, N., Ismail, M., Hanif, A., Farooq, W.A., 2019. Application of silver oxide nanoparticles for the treatment of cancer. J. Mol. Struct. 1189, 203–209. https://doi.org/10.1016/J.MOLSTRUC.2019.04.041.

Ishii, J., Xuan, Y., 2014. Acquirer-target social ties and merger outcomes. J. Financ. Econ. 112, 344–363. https://doi.org/10.1016/J.JFINECO.2014.02.007.

Karpiński, T.M., Adamczak, A., 2017. Antibacterial activity of ethanolic extracts of some moss species. Herba Polonica 63, 11–17. https://doi.org/10.1515/HEPO-2017-0014.

Key, A., Acad, S., Biosci, J., Narasimha Rao, G.M., Jayanth Babu, N.V., Rao, G.M.N., 2022. Scholars Academic Journal of Biosciences Ecological Studies on Bryophytes of Maredumilli Forest Division (AP). Eastern Ghats of India. https://doi.org/10.36347/sajb.2022.v10i03.002.

Khan, M.M., Bhatti, Q.A., Akhlaq, M., Ishaq, M., Ali, D., Jalil, A., Asghar, J., Alarifi, S., Elaissari, A., 2022. Assessment of Antimicrobial Potential of Plagiochasma rupestre Coupled with Healing Clay Bentonite and AGNPS. Biomed. Res. Int. 2022 https://doi.org/10.1155/2022/4264466.

Li, C., Zhang, Y., Wang, M., Zhang, Y., Chen, G., Li, L., Wu, D., Wang, Q., 2014. In vivo real-time visualization of tissue blood flow and angiogenesis using Ag2S quantum dots in the NIR-II window. Biomaterials 35, 393–400. https://doi.org/10.1016/J.BIOMATERIALS.2013.10.010.

Madejová, J., Kečkéš, J., Pálková, H., Komadel, P., 2002. Identification of components in smectite/kaolinite mixtures. Clay Miner. 37, 377–388. https://doi.org/10.1180/0009855023720042.

Mccleary, J.A., Sypherd, P.S., Walkington, D.L., 1960. Mosses as possible sources of antibiotics. Science (1979) 131, 108. Doi: 10.1126/SCIENCE.131.3393.108.

Motti, R., Di Palma, A., de Falco, B., 2023. Bryophytes Used in Folk Medicine: An Ethnobotanical Overview. Horticulturae 2023, Vol. 9, Page 137 9, 137. Doi: 10.3390/HORTICULTURAE9020137.

Mukhia, S., Mandal, P., Singh, D.K., Singh, D., 2019. Comparison of pharmacological properties and phytochemical constituents of in vitro propagated and naturally occurring liverwort Lunularia cruciata. BMC Complement. Altern. Med. 19 https://doi.org/10.1186/S12906-019-2534-4.

Munir, T., Mahmood, A., Fatima, S., Sohail, A., Fakhar-e-Alam, M., Atif, M., Rafaqat, N., 2023. Structural, optical and thermoelectric properties of (Al and Zn) doped Co9S8-NPs synthesized via co-precipitation method. J. King Saud Univ. Sci. 35 https://doi.org/10.1016/J.JKSUS.2023.102836.

Ndikau, M., Noah, N.M., Andala, D.M., Masika, E., 2017. Green Synthesis and Characterization of Silver Nanoparticles Using Citrullus lanatus Fruit Rind Extract. Int. J. Anal. Chem. 2017 https://doi.org/10.1155/2017/8108504.

Ngulube, T., Gumbo, J.R., Masindi, V., Maity, A., 2017. An update on synthetic dyes adsorption onto clay based minerals: A state-of-art review. J. Environ. Manage. 191, 35–57. https://doi.org/10.1016/J.JENVMAN.2016.12.031.

Odom, I.E., 1984. Smectite clay minerals: properties and uses. Philos. Trans. R. Soc. Lond. 391–409 https://doi.org/10.1098/RSTA.1984.0036.

Park, M.H., Valan Arasu, M., Park, N.Y., Choi, Y.J., Lee, S.W., Al-Dhabi, N.A., Kim, J.B., Kim, S.J., 2013. Variation of glucoraphanin and glucobrassicin: anticancer components in Brassica during processing. Food Sci. Technol. 33, 624–631. https://doi.org/10.1590/S0101-20612013000400005.

Rucha, D., Bhavn…, M.K., Jha, P.K., Desai, R., Mankad, V., Gupta, S.K., 2012. Size distribution of silver nanoparticles: UV-visible spectroscopic assessment. ingentaconnect.comR Desai, V Mankad, SK Gupta, PK JhaNanoscience and nanotechnology letters, 2012•ingentaconnect.com 4, 30–34. Doi: 10.1166/nnl.2012.1278.

Sabovljevic, A., Sokovic, M., Sabovljevic, M., Grubisic, D., 2006. Sabovljevic). Fitoterapia 77, 144–145. https://doi.org/10.1016/j.fitote.2005.11.002.

Saritas, Y., Sonwa, M.M., Iznaguen, H., König, W.A., Muhle, H., Mues, R., 2001. Volatile constituents in mosses (Musci). Phytochemistry 57, 443–457. https://doi.org/10.1016/S0031-9422(01)00069-3.

Sharma, V.K., Yngard, R.A., Lin, Y., 2009. Silver nanoparticles: Green synthesis and their antimicrobial activities. Adv. Colloid Interface Sci. 145, 83–96. https://doi.org/10.1016/J.CIS.2008.09.002.

Srivastava, S., Bhargava, A., 2022. Biological Synthesis of Nanoparticles: Bryophytes. Green Nanoparticles Future Nanobiotechnol. 173–180 https://doi.org/10.1007/978-981-16-7106-7_8.

Wiegand, C., Abel, M., Ruth, P., Elsner, P., Hipler, U.C., 2015. pH Influence on Antibacterial Efficacy of Common Antiseptic Substances. Skin Pharmacol. Physiol. 28, 147–158. https://doi.org/10.1159/000367632.

Ying, S., Guan, Z., Ofoegbu, P.C., Clubb, P., Rico, C., He, F., Hong, J., 2022. Green synthesis of nanoparticles: Current developments and limitations. Environ. Technol. Innov. 26, 102336 https://doi.org/10.1016/J.ETI.2022.102336.

Zhang, X.F., Liu, Z.G., Shen, W., Gurunathan, S., 2016. Silver Nanoparticles: Synthesis, Characterization, Properties, Applications, and Therapeutic Approaches. International Journal of Molecular Sciences 2016, Vol. 17, Page 1534 17, 1534. Doi: 10.3390/IJMS17091534.

Zhang, X., Zhao, Y., Wang, S., 2017. Responses of antioxidant defense system of epilithic mosses to drought stress in karst rock desertified areas. Acta Geochim. 36, 205–212. https://doi.org/10.1007/S11631-017-0140-Z.

Zhao, X., Liu, W., Cai, Z., Han, B., Qian, T., Zhao, D., 2016. An overview of preparation and applications of stabilized zero-valent iron nanoparticles for soil and groundwater remediation. Water Res. 100, 245–266. https://doi.org/10.1016/J.WATRES.2016.05.019.

Zielińska, A., Skwarek, E., Zaleska, A., Gazda, M., Hupka, J., 2009. Preparation of silver nanoparticles with controlled particle size. Procedia Chem. 1, 1560–1566. https://doi.org/10.1016/J.PROCHE.2009.11.004.